General Disclaimer

One or more of the Following Statements may affect this Document

- This document has been reproduced from the best copy furnished by the organizational source. It is being released in the interest of making available as much information as possible.

- This document may contain data, which exceeds the sheet parameters. It was furnished in this condition by the organizational source and is the best copy available.

- This document may contain tone-on-tone or color graphs, charts and/or pictures, which have been reproduced in black and white.

- This document is paginated as submitted by the original source.

- Portions of this document are not fully legible due to the historical nature of some of the material. However, it is the best reproduction available from the original submission.

Ohio State University

#6

N70-13407

Progress Report

OSURF Project No. 2792

NASA Grant No. NGR 36-008-109

Period ending 6-30-69

Flutter of Thermally Stressed

Plates at Hypersonic Speeds

Introduction

In a recent paper (attachment No. 1), it was shown that the coupled dynamic response of thermally stressed plates depend primarily upon two factors:

a) the thermal buckling eigenvalues (critical thermal loading) of the idealized perfect plate and,

b) the initial deformation of the mid-plane of the real plate.

The eigen values may be obtained analytically only after the thermal stress distribution has been found. Attemps to determine the critical temperatures experimentally have been unsuccessful because real plates are not perfect plates. Coupling between modes causes the imperfections to affect the rate of change of stiffness thus causing extrapolation of experimental data to lead to erroneous results.

The initial deformation may be measured; however, only quantitative experimental data on the effects of initial deformation have been obtained to date. At the suggestion of the project monitor, an experimental program is being initiated from which it is expected that quantitative data will be obtained to substantiate the theoretical results.

The effort reported herein is an investigation of various

Code-15

Page - 33

Cat - 32

approximate solutions to the thermal stress problem with mixed boundary conditions. The usual procedure is to ignore the clamped edge effect when investigating stresses and thus treat the problem as though the boundary conditions are uniform. For small aspect ratios, however, the influence of the root region may extend over the entire plate. For large aspect ratios the longitudinal stress dominates while for small aspect ratios the transverse stress will dominate. Thus, the complete stress distribution must be known with some confidence as to its accuracy, if the eigen-values are to be accurately determined.

A survey of the literature has revealed that very little work has been reported on efforts to solve this mixed boundary value problem. An exact solution does not appear possible. Thus, the problem becomes that of either evaluating existing methods of approximate solutions or developing new or modified methods to give suitable accuracy.

A method of solution for the equivalent deflection problem is suggested by Timoshenko[1]*, but the tabular results given are from a finite difference solution for the equivalent of a constant temperature. The only other solution found[2] gives a stress concentration at the clamped corner of approximately $10 E \alpha T_o$. This is unreasonably large; also, the method is not readily adaptable to variable planform and variable thickness. The lack of data in this area raises two pertinent questions:

1) "What do the various approximate methods yield for the stress distribution in a cantilever plate?"

---

*( ) refers to references listed on Page 14

2) "Which method will be best suited for the project at hand and why?"

An article published about plate deflections in the AIAA Journal, May, 1969,[3] substiantiates many of the conclusions reached in this investigation. However, several conclusions reached herein go beyond the scope of that article.

The approximate methods of solution under investigation are:

a) Complementary energy,

b) Complementary energy with constraints,

c) Collocation with constraints, and

d) Point matching.

Data to which comparisons are made were obtained from existing solutions by finite differences for a uniform temperature increase,[4] a matrix finite element displacement solution for an experimentally measured temperature distribution and stresses from measured strains for the same experimental temperature distribution[5]. Also, where applicable the results for the stresses in a free plate under a parabolic temperature distribution[6] have been compared.

Because of different planform geometries and temperature distributions used in the existing solutions, manpower and time have not permitted all of the methods investigated to be compared on a common basis. However, it is felt that sufficient data have been obtained to justify the conclusions reached.

Discussion

a) Complementary energy without constraints

In this, the classical method of complementary energy, a stress function that satisfies the stress boundary conditions is assumed.

For a plate symmetrical about the ξ axis with all boundaries free, such a function is:

$$F = (1-\xi^2)^2 (1-\eta^2)^2 \sum_p \sum_q C_{pq} \xi^p \eta^q$$

with both p and q even integers. For the cantilever plate, such a function which satisfies the stress free conditions on only three edges is:

$$F = (1-\xi)^2 (1-\eta^2)^2 \sum_p \sum_q C_{pq} \xi^p \eta^q .$$

where p includs both even and odd integers while q is still restricted to even integers only.

On applying the Rayleigh-Ritz technique to the complementary energy, the C_{pq} may be determined for a given temperature distribution. The stresses are then given by:

$$\sigma_\xi = \frac{\partial^2 F}{\partial \eta^2}$$

$$\sigma_\eta = \frac{\partial^2 F}{\partial \xi^2}$$

$$\tau_{\xi\eta} = -\frac{\partial^2 F}{\partial \xi \partial \eta}$$

Several terms are required to give a solution that is sufficiently converged in all three stresses. In fact, the solution changes so drastically with the first few terms as to give the impression that the solution is divergent. However, it appears to converge satisfactorily at every point except in the immediate

neighborhood of the boundary discontinuity at the clamped corner.

A sixteen term solution using the available experimental temperature distribution[5] was obtained and is compared to the referenced data, Fig. 1, for a rectangular plate, and Fig. 2, for a triangular plate.

Based on these comparisons, it is concluded that the Rayleigh-Ritz technique applied to the complementary energy yields the proper functional form of the longitudinal stress distribution and reasonably close magnitudes of the stresses in the body of both rectangular and tapered plates. Similar experimental data for comparison of the lateral stress are not available. The resulting lateral stress from the complementary energy is compared to other theoretical methods as they develop.

Since the finite element matrix displacement method in effect satisfies the displacement boundary conditions, it may be assumed that that solution is reasonably close to the actual stresses in the neighborhood of the root. Since at the point, $\xi = .06$, $\eta = .17$ the complementary energy solution is reasonably close to the matrix displacement solution, it would appear that the energy solution may be reasonably close in the neighborhood of the root.

The stresses as obtained from the energy solution do not satisfy the displacement boundary conditions, $\epsilon_1 = \frac{\partial V}{\partial \eta} = 0$ or $V = 0$, at the root. A plot of $\epsilon_\eta / \alpha T_0$ at $\xi = 0$ for the 16-term solution with experimental temperature is shown in Fig. 3. Also, in the same figure is shown a plot of the strain ratio, $\epsilon_\eta / \alpha T_0$, for a parabolic temperature distribution, which is equivalent to free expansion in the η direction at $\xi = 0$.

b) Complimentary Energy with Constraints

In an effort to more closely satisfy the displacement boundary conditions, these conditions were written in terms of the stresses and the resulting equations used as equations of constraint by the Lagrangian multiplier technique. Fig. 4 shows that the desired results were very nearly achieved in so far as the displacements are concerned. However, the solution did not converge with 24 terms in the stress function. Experience with the collocation method and with this method indicates that the stress results are inconclusive. Convergence may occur with the addition of higher order terms, provided numerical instability is not encountered in the computational program before sufficient terms can be included.

c) Collocation with Constraints

An integrodifferential equation on the shear stress was derived as for a free plate in NACA TN D-1182[6]. Again the displacement boundary conditions were expressed in terms of the stresses and these equations were then used to satisfy these boundary conditions at points on the fixed boundary. The integrodifferential equation was satisfied at points on the free boundary and at points on the interior of the plate. Solutions were obtained for both a uniform temperature and a parabolic temperature distribution.

The collocation results for the longitudinal stress in Fig. 5 may be compared to the classical complimentary energy solution for a parabolic temperature in Fig. 6. Note that the area of disagreement is in the root region, $\xi \leq .3$. But note that even in this region the general shape of the curves are the same except for $\eta = .9$.

Fig. 7 and Fig. 8 shows the transverse stresses for the case of a parabolic temperature. Note that the complementary energy compares favorably with the collocation method. Fig. 9 shows a comparison of the strains as calculated from both methods. Note that the collocation method very nearly satisfies the displacement boundary condition, V = .0, in the mean while the energy method does not. Fig. 10 shows the transverse stress due to a uniform temperature rise in a rectangular plate. In this case, the only stresses in the plate are those caused by the clamped boundary. Note the close agreement between the three solutions shown.

d) Point Matching

This method was applied to the mixed boundary condition problem for this project by Professor Buford E. Gatewood. In it, the bi-harmonic stress equation is satisfied exactly in the interior of the plate. The shear boundary condition is satisfied exactly on the free edge while the normal stress boundary condition is satisfied at selected points. On the fixed edge the displacement condition, $\frac{\partial^2 U}{\partial \eta^2}$, is satisfied exactly while the strain condition, $\frac{\partial v}{\partial \eta}$, is satisfied at selected points.

Results have been obtained for $AR = 1$ and a uniform temperature change. It compares favorably with an unpublished finite difference solution[4] except at the fixed corner of the plate where the boundary discontinuity occurs. Since the solution involves hyperbolic and trigonometric functions it does not appear readily adabtable to variable planforms and thicknesses. However, further work may be of academic interest for the purpose of com-

parison of the root region with other solutions.

Conclusions

The advantages and disadvantages of the complementary energy solution are:

a) The thermal loading term permits integration of the temperature function. This is a very definite advantage when considering experimentally determined temperature distributions.

b) Formal integration may be applied to evaluate the elements of the complementary energy matrix, thus cutting computer time by more than an order of magnitude when compared to numerical integration. This factor is normally listed as a disadvantage of the energy method because the formal integration is extremely tedious.

c) Variable planform geometry is accounted for in the limits of integration and in the stress function. Thus, a broad class of plates may be treated for a prescriped boundary condition and a given class of geometrical shapes; e.g., the integrals for the class of symmetrically tapered cantilever plates of constant thickness have already been evaluated.

d) Variable thickness may be accounted for by its inclusion in the integrand. If it can be expressed as a polynomial, the integrals for constant thickness appear to be readily adaptable to yield the correct values without further integration. However, computer time will be increased accordingly.

e) Regardless of how the stresses are found, the determination of the thermal buckling eigen values requires the evaluation of an integral representing the energy due to the stresses:

$$\iint \left\{ \sigma_\xi \left(\frac{\partial w}{\partial \xi}\right)^2 + \sigma_\eta \left(\frac{\partial w}{\partial \eta}\right)^2 + 2\,\tau_{\xi\eta} \frac{\partial w}{\partial \xi} \frac{\partial w}{\partial \eta} \right\} d\xi\, d\eta$$

On substituting the stress function (see page 4) with known C_{pq} into this integral, the elements of the matrix representing this energy may be obtained by formal integration in terms of the exponents of the polynomial representing the deflection function, W. This integral is most difficult to determine accurately and is very time consuming if done by numerical integration. It is expected that formal integration will reduce the computer time by again more than an order of magnitude when compared to numerical integration with the necessary double precision.

f) The primary disadvantage of the energy approach appears to be that it may not give a sufficiently close approximation to the stress in the immediate neighborhood of the plate root. However, comparison with other methods indicates that the general shape of the stress distribution in this region must be about right except possibly in the neighborhood of the boundary discontinuity. The eigen values depend only on the functional form or shape of the stress distribution and not on its magnitude. Thus, the eigen values as determined from the complimentary energy stresses

are expected to be sufficiently accurate.

g) Normally, a disadvantage of the complementary energy method would be the large number of terms required. However, formal integration has made possible the complete stress distribution (three stresses at 121 points) for 16 terms, double precision, in .3 minutes on an IBM 360, Model 75 computer. A 24 term solution, double precision, requires thirty seconds.

Both the collocation with constraints and the point matching techniques readily yield stresses for the rectangular plate of constant thickness and one would expect, on the basis of more closely satisfying the displacement boundary conditions, that the stresses except in the neighborhood of the boundary discontinuity will be very nearly correct. However, neither method is as readily adaptable to variable planform and variable thickness as is the complementary energy.

Both the finite element matrix displacement method and the method of finite differences yield accurate stress distributions except at the boundary discontinuity. However, the use of numerical stresses as produced by these methods requires numerical integration of the elements of the mid-plane energy matrix, a time consumming process for the computer.

Based upon the foregoing investigation, the complementary energy method will be used for the thermal stress determination for this project. It is hoped that time will permit a comparison of the results for all the methods on the basis of common geometry and a common temperature distribution. This, combined with substantiating experimental evidence of the stresses in the root

region and along the plate edge should result in a worthwhile paper of some practical value.

Future Effort

The stress problem is a necessary by-product of the primary investigation of this project. It is felt that the primary effort must be exerted in such a way as to lead to answers to the problem of the flutter of plate lifting surfaces at hypersonic speeds. Toward this end, the following efforts are under way:

I. Continuing investigation of stresses to include non-symmetrical plates of variable thickness. This effort is ultimately to lead to computer programs from which both thermal buckling eigen values and vibration frequencies may be obtained. This information is basic to the prediction of flutter.

II. Experimental determination of the initial shape parameters, ϕ_i and ψ_i, for a rectangular plate and comparison of the experimental behavior of the plate to that predicted by the non-linear theory when the measured shape parameters are used. This will show that the behavior of a particular plate may indeed be quantitatively predicted.

III. Experimental investigation of the stress along the free edge and in the neighborhood of the root of a thermally stressed cantilever plate. From the theory there appears to be a wave in the magnitude of the longitudinal stress along the edge. This wave does not appear in the free plate and disappears by one tenth of the semi-chord from the edge in the cantilever plate. Is this stress wave actually present or is it a pecularity of the stress function? It is hoped that a few strategically placed strain gages with some thought given to producing the

correct boundary conditions will yield convincing results as well as results on the transverse stress.

IV. Derivation of the equations for two-dimensional flutter of a thermally stressed plate at hypersonic speed using piston theory. On obtaining these equations, a parametric study may be accomplished wherin it is hoped that the relations between various parameters necessary for instability will be revealed. Following this study and the completion of item I, the flutter of specific lifting surfaces may be undertaken.

References:

1. Timoshenko, S. and Woinowsky-Krieger, "Theory of Plates and Shells", 2nd Ed., McGraw-Hill Book Company, Inc., New York, N.Y. P. 211.

2. Aleck, B.J., "Thermal Stresses in a Rectangular Plate Clamped Along an Edge". Journal of Applied Mechanics, Vol. 16, No. 2, June, 1949, P. 118.

3. Lissa, A W., Clausen, W.E , Hulbert, L.E., and Hopper, A.T., "A Comparison of Approximate Methods for the Solution of Plate Bending Problems", AIAA Journal, Vol. 7, No. 5, May 1969. P. 920.

4. Gatewood, B. E. "Thermal Stresses due to a Uniform Temperature Change in a Rectangular Plate Clamped Along One Edge by the Method of Finite Differences" Unpublished data.

5. DeSantis, Joseph G., "Experimental Thermal Stresses in Cantilevered Trapezoidal Plates", Master of Science Thesis, The Air Force Institute of Technology, Wright-Patterson Air Force Base, Ohio, June 1967, Unpublished.

6. Roberts, Ernest, Jr., "Elastic Design Charts for Thin Plates With Spanwise and Chordwise Variations in Temperature", NACA TN D-1182, March 1962.

T = Experimental

Rectangular Plate

Aspect Ratio = 5/3

Rayleigh-Ritz ——

Finite Element ⊡

Experimental ⊗

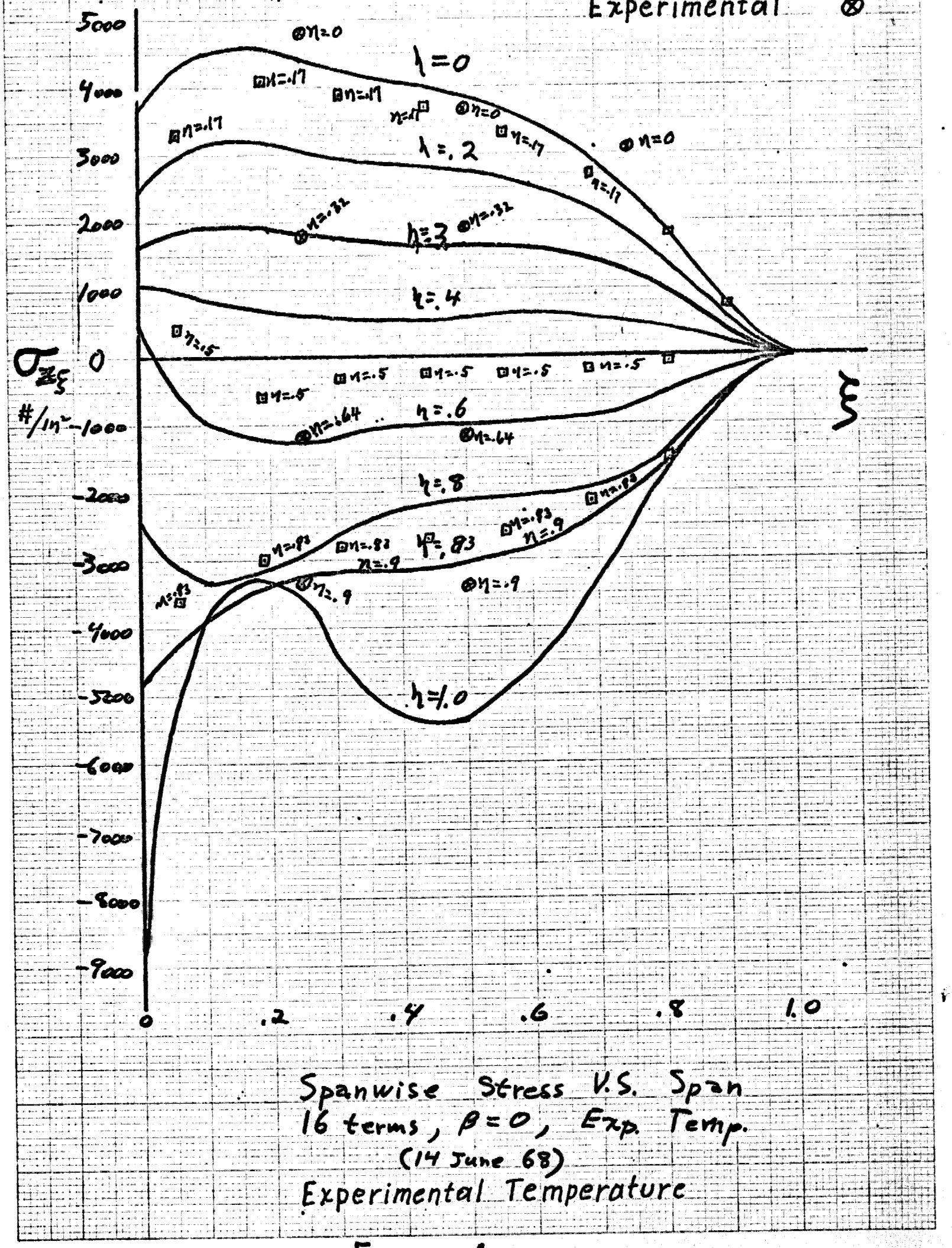

Spanwise Stress V.S. Span

16 terms, β=0, Exp. Temp.

(14 June 68)

Experimental Temperature

Figure 1

Triangular Plate
Aspect Ratio = 5/3

Rarleigh Ritz
Finite Element
Experimental

6,000
4,000
2,000
σ_ξ, #/in² 0
2,000
4,000
6,000
8,000

σ_ξ Stress on Plate edge

0 .2 .6 .8 1.0 ξ

↓ 18,800 @ η=1.0

Spanwise Stress Vs. Span
Experimental Temperature

Figure 2

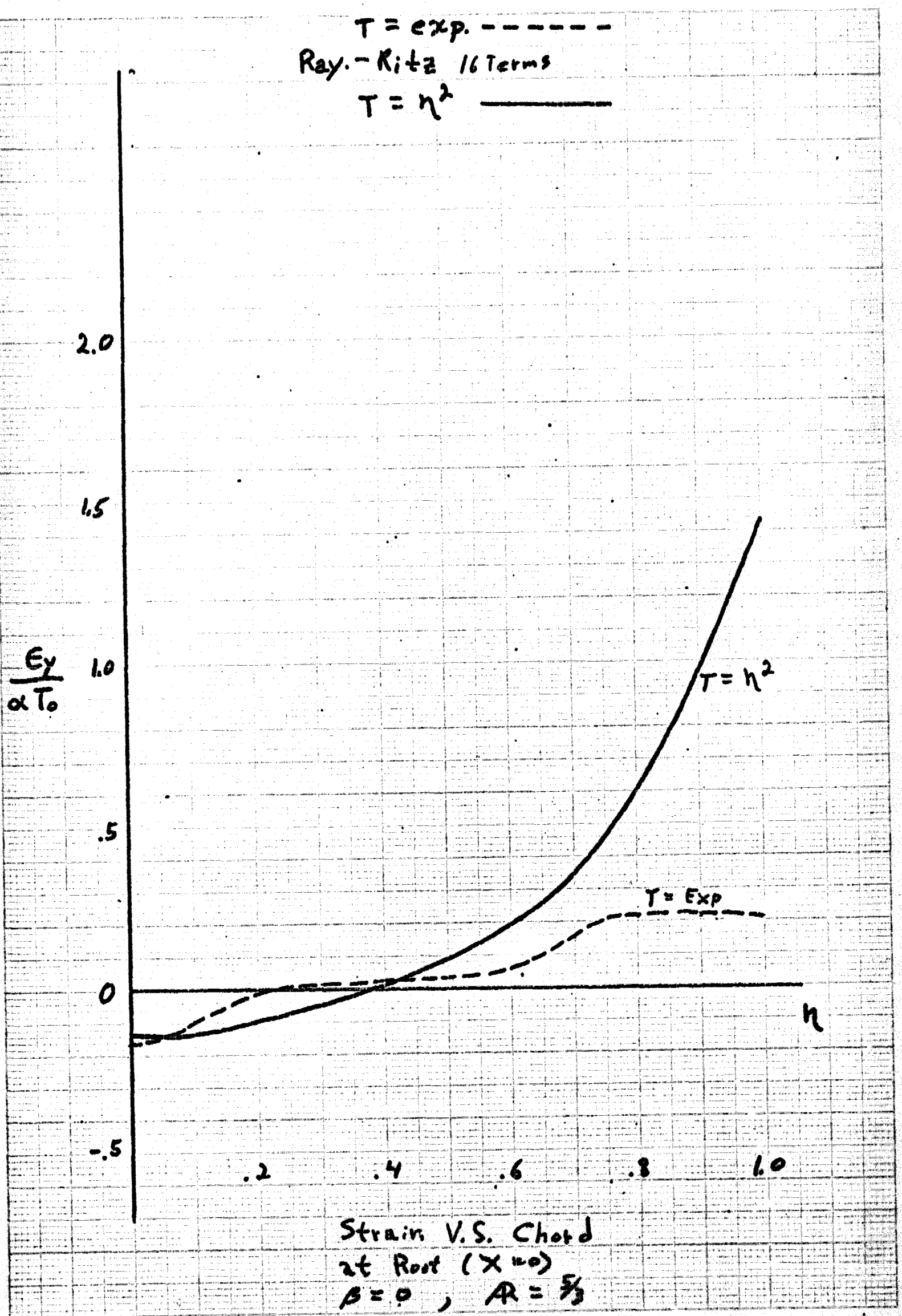

Strain V.S. Chord
at Root (X = 0)
β = 0 , AR = 5/3

Figure 3

$\tau = \eta^2$

Ray.- Ritz

(16 Terms)

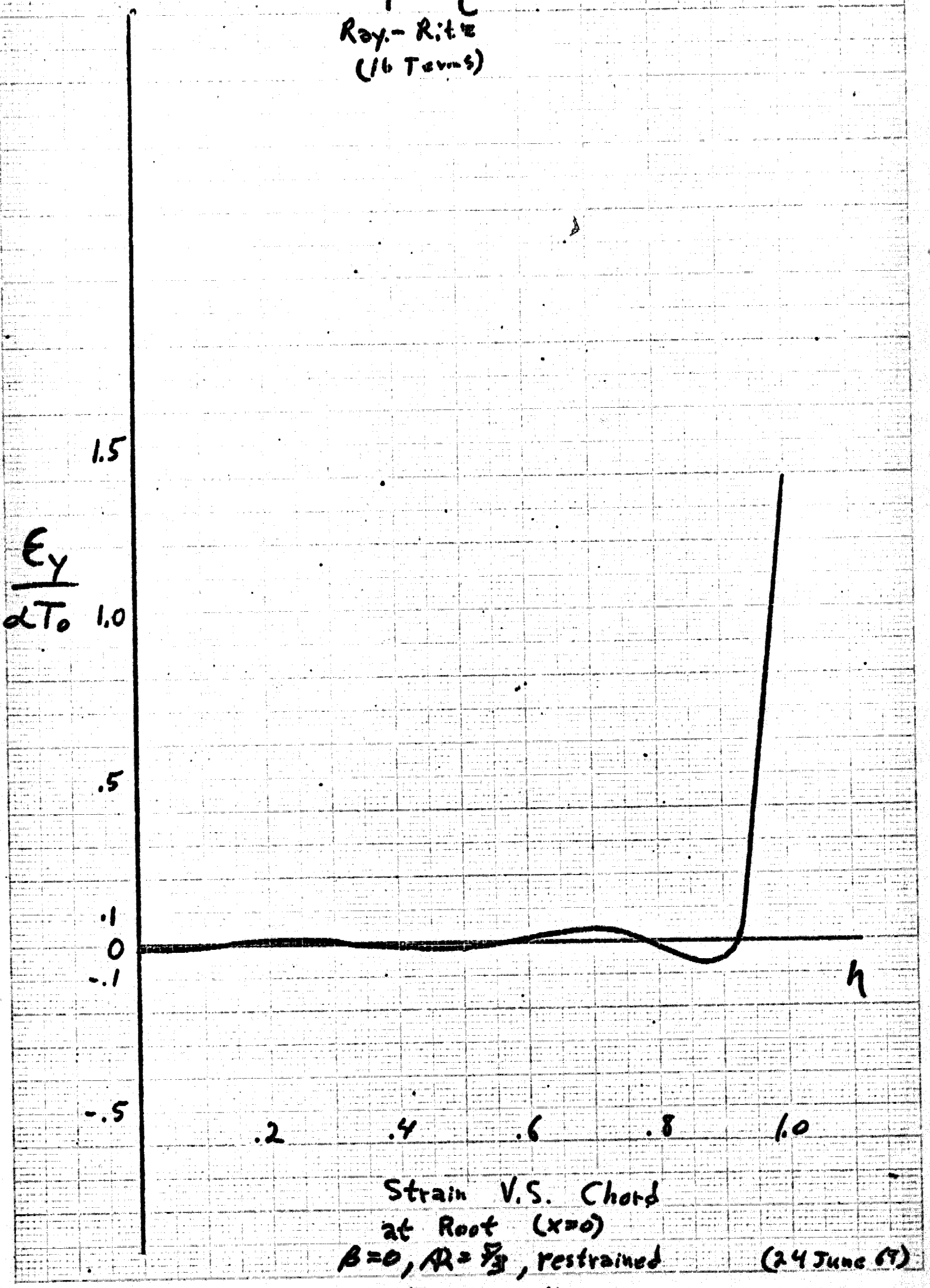

Strain V.S. Chord

at Root (x=0)

$\beta = 0$, $AR = \frac{5}{3}$, restrained (24 June 57)

Figure 4

4 × 10 COLLOCATION

$B = 0$

$T = T_0 \tilde{\zeta}^2$

$\tilde{\zeta}$ ~ DIMENSIONLESS CHORD COORDINATE

$\eta = 0$

.2

.4

.5

.6

.7

.8

.9

1.0

-502

DIMENSIONLESS STRESS ~ $\frac{\sigma_x}{T_0}$ ~

60

40

20

0

-20

-40

-60

-80

-100

SPANWISE COORDINATE ~ $\tilde{s}$ ~

0 .2 .4 .6 .8 1.0

Figure 5

$T = \eta^2$

16 TERMS

$\beta = 0$

$T = T_0 \eta^2$

η ~ DIMENSIONLESS CHORD COORDINATE

60

40

20

0

-20

-40

-60

-80

-100

-102

$\eta = 0$

.2

.4

.5

.6

.7

.8

.9

1.0

ξ

DIMENSIONLESS STRESS ~ $\frac{\sigma_x}{D T_0}$

SPANWISE COORDINATE ~ ξ ~

0 .2 .4 .6 .8 1.0

Figure 6

$T = (\beta)^2 = \eta^2$

Collocation

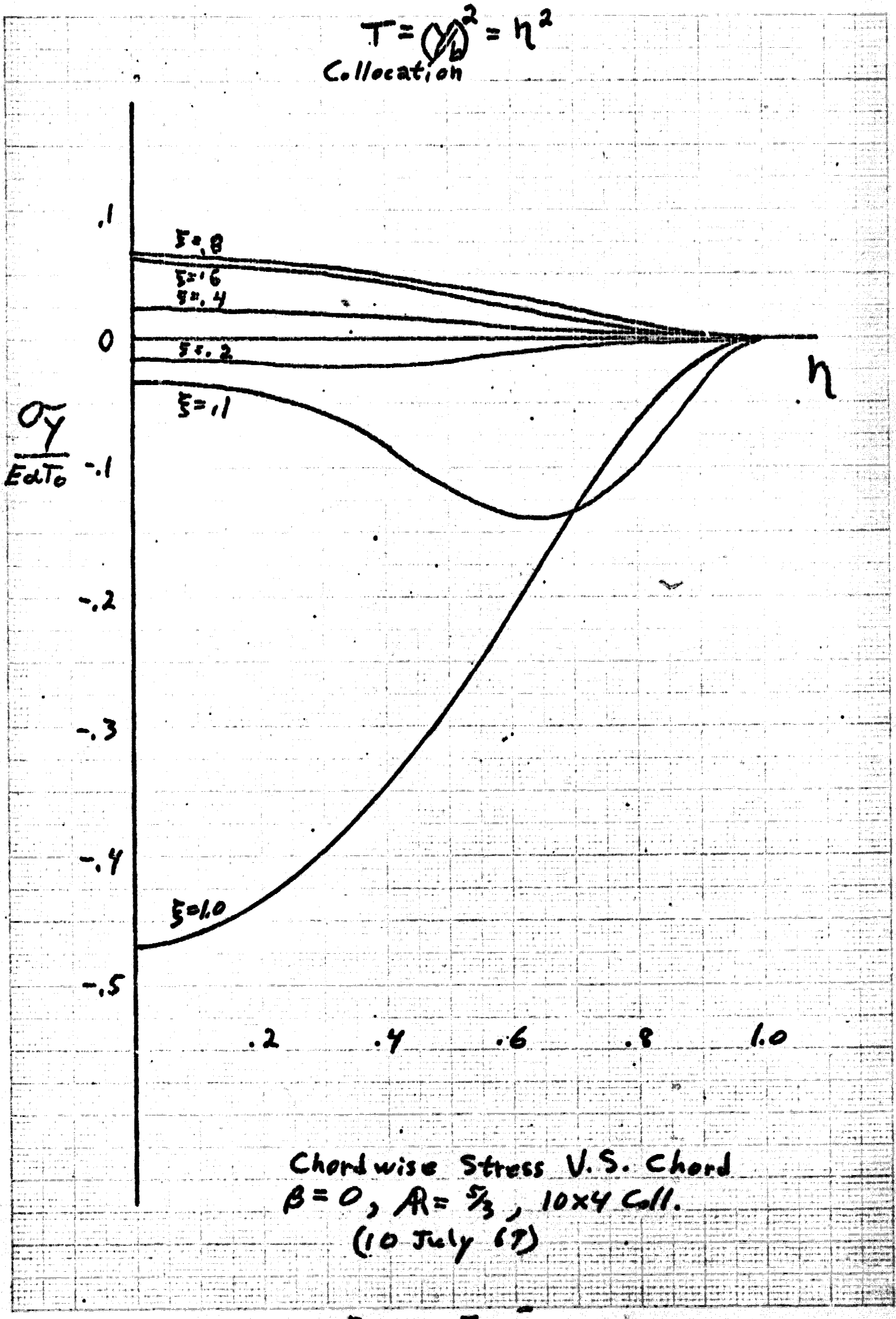

Chordwise Stress V.S. Chord
$\beta = 0$, $AR = 5/3$, 10x4 Coll.
(10 July 67)

Figure 7

$T = (\gamma_b)^2 = \eta^2$

Ray.-Ritz 2. 16 Terms

(20 Sept 68)

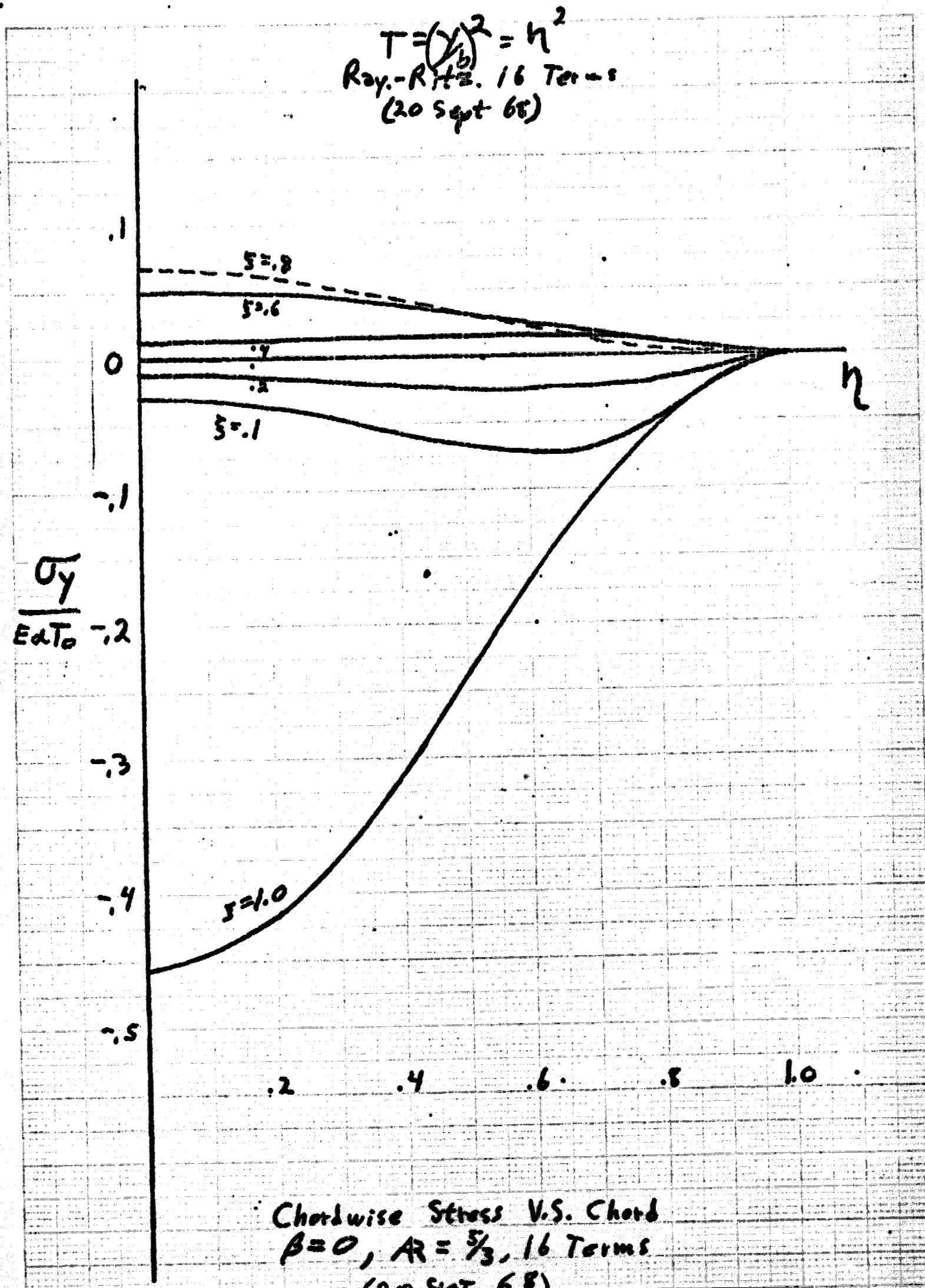

Chordwise Stress V.S. Chord

$\beta = 0$, $AR = 5/3$, 16 Terms

(20 Sept 68)

Figure 8

$$T = \left(\frac{y}{b}\right)^2 = \eta^2$$

Rzy.-Ritz. (20 sept 68) - - - -

Collocation (10 July 69) ——

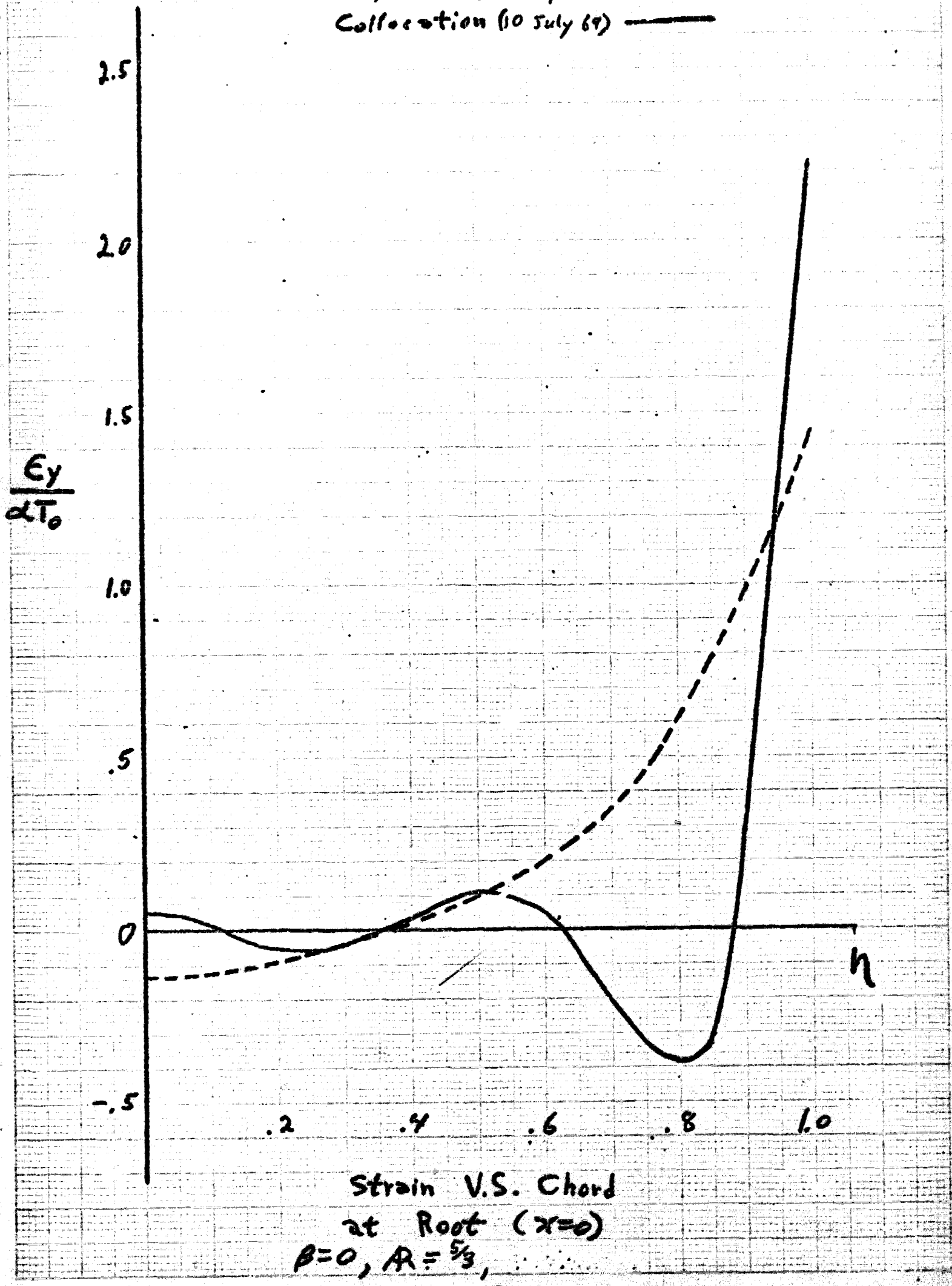

Strain V.S. Chord
at Root ($x=0$)
$\beta=0$, $A=5/3$, ...

Figure 9

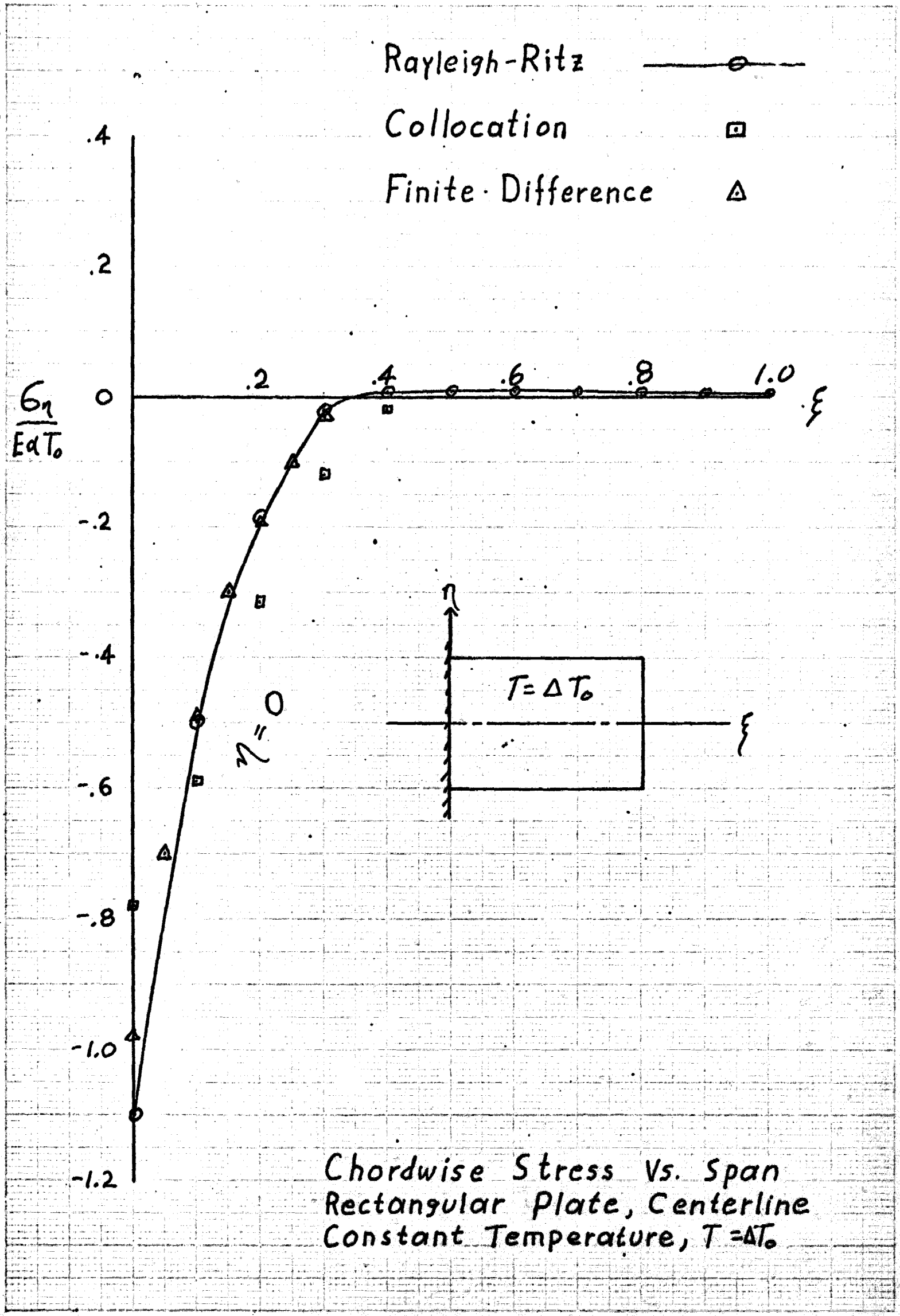

Chordwise Stress Vs. Span
Rectangular Plate, Centerline
Constant Temperature, $T = \Delta T_o$

Figure 10

MODAL COUPLING IN THERMALLY STRESSED PLATES*

Attach. #1

Cecil D. Bailey
The Ohio State University

Abstract

An approximate, but general, solution for the frequencies, thus the effective stiffnesses, in the first and second modes of initially deformed, thermally stressed plates of any planform shape and with any boundary condition is found in terms of quantities that may be obtained from the application of linear theory.

It is shown that all plates exhibit the same characteristic changes in frequency, thus stiffness, independent of planform shape, boundary conditions and temperature distribution except as these factors affect the thermal buckling eigenvalues (ΔT critical).

Coupling between the modes is shown to depend upon the ratio of the thermal buckling eigenvalues; but, initial deflection in one mode will affect the other mode even in the case of artificial uncoupling.

Both analytical and experimental data are presented to show that the second mode stiffness for cantilever plates does not always increase in the post buckled region as implied in the literature; but, depending upon the ratio of the buckling eigenvalues and upon the initial displacements, the second mode will level off at some minimum frequency while the first mode frequency increases. Conversely, when the second mode increases, the first mode levels off at some minimum.

List of Symbols

B	Normal coordinate for the first mode
C	Large deflection stress function parameter
D.	Plate stiffness, $Et^3/12(1-\nu^2)$
E	Modulus of elasticity
F	Large deflection stress function
G	Small deflection stress function
$I_1, \ldots, I_9$	Definite integrals involving functions W_1, W_2 and G.
I_{10}	Work done by the stress over that part of the boundary on which the displacements are prescribed.
T	Temperature distribution over the surface of the plate.
ΔT_B	Reference temperature at which buckling in first mode occurs.
ΔT_T	Reference temperature at which buckling in second mode occurs.
t	Plate thickness
$\bar{U}$, $\bar{V}$	Displacement in the x and y directions respectively on that part of the boundary where the displacements are prescribed.
W	Total displacement of elastic surface from the x, y plane
W_i	Initial displacement of elastic surface from the x, y plane. Also called initial imperfection and/or initial deformation.
W_1	First mode from linear solution.
W_2	Second mode from linear solution.
Z	Sum of forces per unit area normal to the plane of the plate, $P(x, y) - \rho t\ddot{W}$.
P(x, y)	Applied load over plate surface. May also be a function of time.
α	Thermal coefficient of expansion.
Γ	Energy due to heating, $\iint t\alpha T(\sigma_x^2 + \sigma_y^2)dxdy$.
Γ_B	Value of Γ at which the perfect, unloaded plate would buckle in the first mode.
Γ_T	Value of Γ at which the perfect, unloaded plate would buckle in the second mode.
ϵ_x	Small amplitude dynamic displacement of first mode.
ϵ_ϕ	Small amplitude dynamic displacement of second mode.
θ	Normal coordinate for second mode.
ν	Poisson's ratio.
τ	Time.
ϕ	Non-dimensionalized normal coordinate for second mode.
ψ	Non-dimensionalized normal coordinate for first mode.

*Supported in part by the Air Force Institute of Technology and by the Office of Aerospace Research, USAF.

ϕ — Non-dimensional large static deflection, second mode.

Ψ — Non-dimensional large static deflection, first mode.

ω — Frequency of small amplitude vibration about large amplitude static equilibrium position.

ω_{o_B} — First mode, free vibration frequency, at uniform temperature.

ω_{o_T} — Second mode, free vibration frequency, at uniform temperature.

Introduction

Heldenfels and Vosteen[2] showed that the torsional frequency and stiffness of a thermally stressed cantilever plate always increases after reaching some minimum. The minimum stiffness is dependent upon the initial deformation. The solution obtained is shown in Figure 1, where the curve parameter ϕ_1 is a measure of the initial twist in the plate.

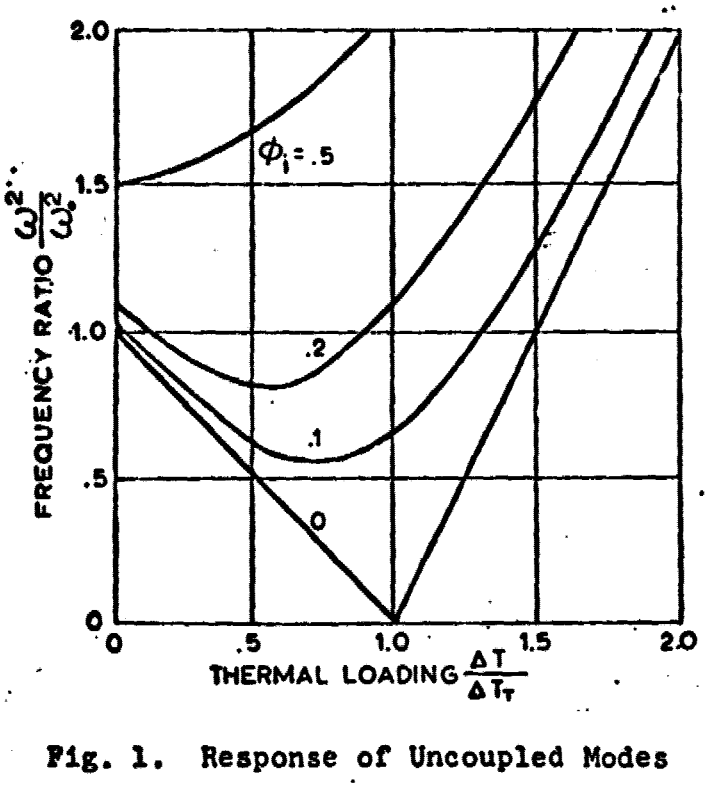

Fig. 1. Response of Uncoupled Modes

They tested a square cantilever plate which had initial deformation in both the symmetrical (bending) mode and antisymmetrical (torsion) mode. The plate and its initial shape are shown in Figure 2. Their plot of experimental data which verified their analytical solution is shown in Figure 3.

Breuer,[4] verified the results of Heldenfels and Vosteen and extended the solution to plates of other aspect ratio.

Bailey,[3] extended the analytical results of Heldenfels and Vosteen and showed that their solution for torsion is also the solution for bending when the two modes are uncoupled. However, in conducting an experimental investigation of tapered plates in the pre-buckled region, it was noted that in those instances when the heat

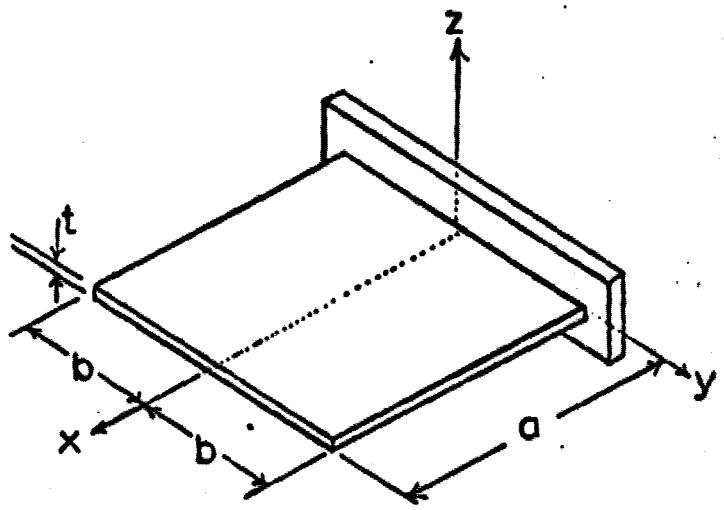

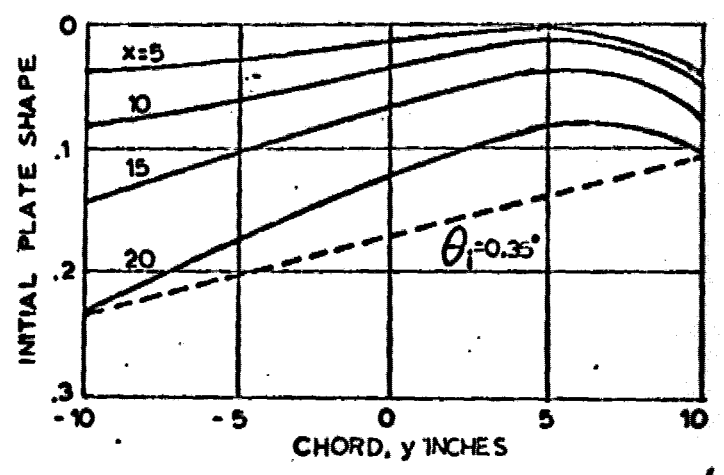

Fig. 2. Initial Plate Shape, NASA Report 1361

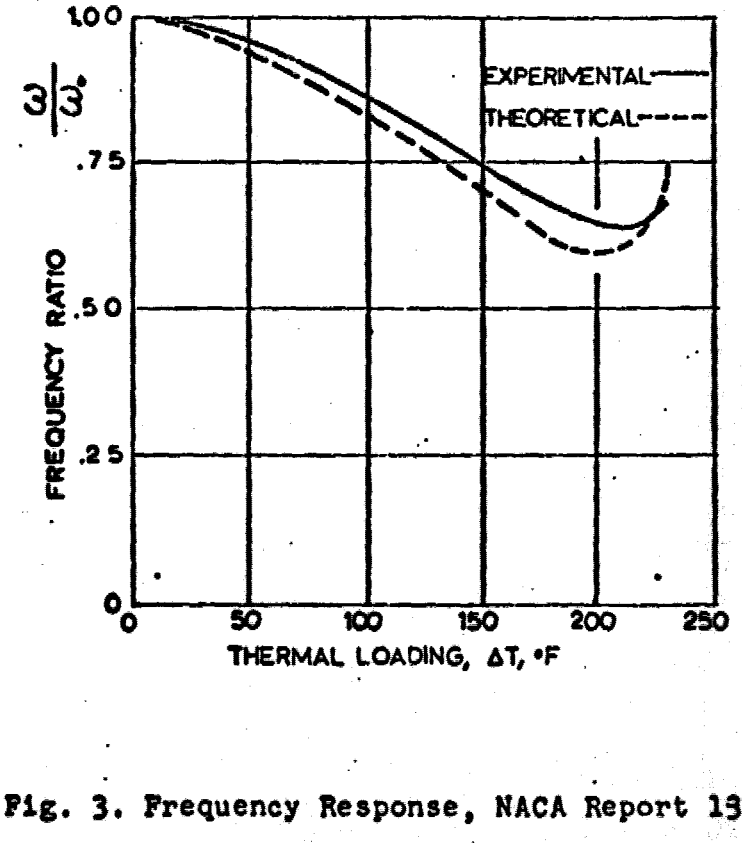

Fig. 3. Frequency Response, NACA Report 1361

was left on longer than usual, the torsional frequency did not increase after reaching a minimum but leveled off, indicating that the stiffening effect as recorded by others was not present. The fully tapered plate was the only exception. A typical curve of the phenomena as noted in Reference 4 is shown in Figure 4. No attempt was made to explain the cause of this phenomena until more recent work was accomplished. That work is reported herein.

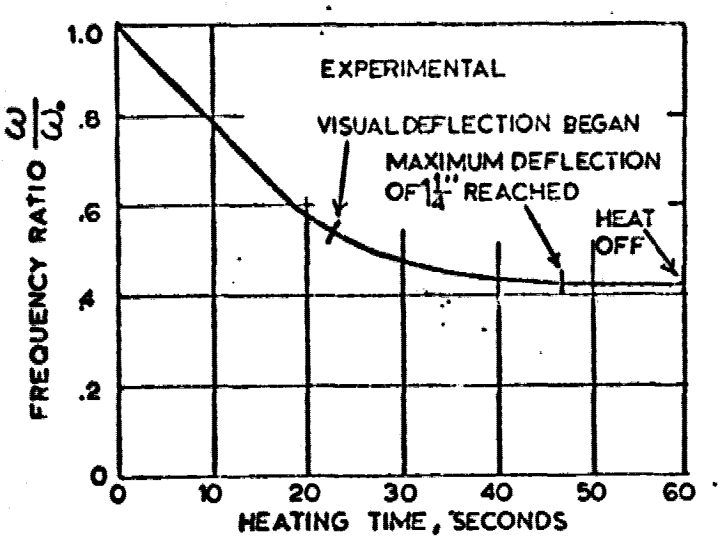

Fig. 4. Frequency Response, Reference 3.

Statement of the Problem and Basic Equations

Given an initially deformed plate of any planform shape, boundary condition, and thickness distribution (provided the thickness distribution permits the assumption of thin plate theory), find the frequency, thus the effective stiffness, when the plate is subjected to thermal stress and large deflections.

Since there is no exact solution to the differential equations of this problem, an approximate solution is obtained by using Reissner's Variational Principle[1] for large deflections:

$$\delta\{\iint[\frac{D}{2}([\frac{\partial^2(W-W_i)}{\partial x^2}]^2 + [\frac{\partial^2(W-W_i)}{\partial y^2}]^2 + 2\nu\frac{\partial^2(W-W_i)}{\partial x^2}\frac{\partial^2(W-W_i)}{\partial y^2} + 2(1-\nu)[\frac{\partial^2(W-W_i)}{\partial x\partial y}]^2) + \frac{t}{2}(\frac{\partial^2 F}{\partial x^2}[(\frac{\partial W}{\partial y})^2 - (\frac{\partial W_i}{\partial y})^2] + \frac{\partial^2 F}{\partial y^2}[(\frac{\partial W}{\partial x})^2 - (\frac{\partial W_i}{\partial x})^2] - 2\frac{\partial^2 F}{\partial x\partial y}[\frac{\partial W}{\partial x}\frac{\partial W}{\partial y} - \frac{\partial W_i}{\partial x}\frac{\partial W_i}{\partial y}]) - \frac{t}{2E}((\frac{\partial^2 F}{\partial x^2})^2 + (\frac{\partial^2 F}{\partial y^2})^2 - 2\nu\frac{\partial^2 F}{\partial x^2}\frac{\partial^2 F}{\partial y^2} + 2(1-\nu)(\frac{\partial^2 F}{\partial x\partial y})^2) - t\alpha T(x,y,\tau)(\frac{\partial^2 F}{\partial x^2} + \frac{\partial^2 F}{\partial y^2})]dxdy - \iint ZWdxdy + \int_c[\frac{\partial^2 F}{\partial y^2}\bar{U} + \frac{\partial^2 F}{\partial x^2}\bar{V}]ds) = 0$$

In the application of this minimal principle the generality of the solution obtained is a result of the functions chosen for the assumed solution. Two functions must be assumed: (1) the deflection function, W, and (2) the stress function, F.

The deflection function is assumed to be,

$$W(x,y,\tau) = B(\tau)W_1(x,y) + \theta(\tau)W_2(x,y)$$

where, $W_1(x,y)$ and $W_2(x,y)$ are the first and second buckling or vibration modes, as determined from the linear solution of whatever plate problem happens to be prescribed. Thus, these functions are orthogonal and satisfy the plate displacement boundary conditions. B and θ are undetermined parameters, in this case normal coordinates for the modes W_1 and W_2. W_i, the initial displacement, is taken to be the same functional form as the large deflection mode

$$W_i(x,y) = B_i W_1(x,y) + \theta_i W_2(x,y)$$

B_i and θ_i are the measured amplitudes that define the magnitude of the initial imperfection.

The stress function for large deflections is assumed to be

$$F = C(\tau)\, G(x,y)$$

where, G(x,y) is the stress function obtained from a linear solution of the stress distribution; thus, it satisfies the stress boundary conditions for whatever planform shape the plate may have. C, B, and θ are undetermined parameters that must be found from the application of Reissner's variational principle.

Substitution of the assumed functions into the variational equation yields three equations in the three unknowns:

$$\ddot{B} + \frac{I_2}{I_1}(B-B_i) + C\frac{I_3}{I_1}B = \frac{I_4}{I_1} \qquad (1)$$

$$\ddot{\theta} + \frac{I_6}{I_5}(\theta-\theta_1) + C\frac{I_7}{I_5} = \frac{I_8}{I_5} \qquad (2)$$

$$C = \frac{I_3}{I_9}(B^2-B_1^2) + \frac{I_7}{I_9}(\theta^2-\theta_1^2) - \frac{\Gamma}{I_9} - \frac{I_{10}}{I_9} \qquad (3)$$

where,

Γ is the thermal loading term.

I_i, i=1,...,9, are definite integrals of the assumed functions and are pure numbers. I_{10} is the work done by the stresses over that part of the boundary where the displacements are prescribed. These integrals are given in Appendix I.

Substitution of the third equation into the first two yields two equations from which B and θ may be determined. From these equations it may be noted that no coupling exists unless large deflections are present; but, if there are finite imperfections then there is a coupling effect even when elastic deflections in a particular mode are artificially prevented.

$$\ddot{B} + B\frac{I_2}{I_1}[1 - \frac{I_3}{I_2I_9}\Gamma - \frac{I_3^2}{I_2I_9}B_1^2 + \frac{I_3I_7}{I_2I_9}(\theta^2-\theta_1^2) - \frac{I_1I_{10}}{I_2I_9}] + \frac{I_3^2}{I_1I_9}B^3 = \frac{I_4}{I_1} + \frac{I_2}{I_1}B_1 \qquad (4)$$

$$\ddot{\theta} + \theta\frac{I_6}{I_5}[1 - \frac{I_7}{I_6I_9}\Gamma - \frac{I_7^2}{I_6I_9}\theta_1^2 + \frac{I_3I_7}{I_6I_9}(B^2-B_1^2) - \frac{I_5I_{10}}{I_6I_9}] + \frac{I_7^2}{I_5I_9}\theta^3 = \frac{I_8}{I_5} + \frac{I_6}{I_5}\theta_1 \qquad (5)$$

As a result of the choice of assumed functions, an examination of the linear equations will show that:

$\frac{I_2}{I_1} = \omega_{o_B}^2$, the first mode, free vibration frequency.

$\frac{I_2I_9}{I_3} = \Gamma_{B_{critical}}$, the first mode, uncoupled, unloaded, perfect plate thermal buckling parameter for the prescribed temperature distribution.

$\frac{I_4}{I_2} = B_o$, the first mode deflection under any applied steady state load normal to the plate surface

$\frac{I_6}{I_5} = \omega_{o_T}^2$, the second mode, free vibration frequency.

$\frac{I_6I_9}{I_7} = \Gamma_{T_{critical}}$, the second mode, uncoupled, unloaded, perfect plate thermal buckling parameter for the prescribed temperature distribution.

$\frac{I_8}{I_6} = \theta_o$, the second mode deflection under the applied steady state load normal to the plate surface.

Now divide equations (4) and (5) by I_2/I_1 and I_6/I_5 respectively, make the foregoing substitutions followed by the following coordinate transformations:

$$\psi^2 = \frac{I_3}{\omega_{o_B}^2\Gamma_B}B^2$$

$$\phi^2 = \frac{I_7}{\omega_{o_T}^2\Gamma_T}\theta^2$$

The resulting equations are:

$$\frac{\ddot{\psi}}{\omega_{o_B}^2} + \psi[1 - \frac{\Gamma}{\Gamma_B} - \psi_1^2 + \frac{\Gamma_T}{\Gamma_B}(\phi^2-\phi_1^2) - \frac{I_{10}}{\omega_{o_B}^2I_9}] + \psi^3 = \psi_o + \psi_1 \qquad (6)$$

$$\frac{\ddot{\phi}}{\omega_{o_T}^2} + \phi[1 - \frac{\Gamma}{\Gamma_T} - \phi_1^2 + \frac{\Gamma_B}{\Gamma_T}(\psi^2-\psi_1^2) - \frac{I_{10}}{\omega_{o_T}^2I_9}] + \phi^3 = \phi_o + \phi_1 \qquad (7)$$

When the displacements over that part of the boundary where the displacements are prescribed are zero, the integral $I_{10} = 0$. Otherwise, it is seen that prescribing boundary displacements will cause the same trend of stiffening as prescribed Γ, ψ_i, or ϕ_i.

It is possible that I_8, I_4, and I_{10} as well as Γ may, any one or all, be functions of time, in which case the problem would be a large amplitude vibration problem under, at most, four different forcing functions.

The assumption is now made that I_4, I_8 and I_{10} are not functions of time and that the rate of change of the displacements as a result of the rate of change of Γ with time is sufficiently slow that the deflections caused by temperature may be treated as a statics problem. Thus, under heat input in the plane of the plate and load normal to the plane, the plate may undergo large static deflections about which small amplitude dynamic oscillations may occur. The square of the frequency of these oscillations is a direct measure of the effective stiffness in the mode and at the displacement under investigation.

To find the frequency of the small amplitude oscillations, let,

$$\psi = c_\psi + \Psi$$

$$\phi = c_\phi + \Phi$$

where

c_ψ and c_ϕ are the small amplitude dynamic displacements, while

Ψ and Φ define the large amplitude static equilibrium position of the respective modes.

Substitution of these definitions into equations (6) and (7) produces (see Appendix II) two equations for the frequencies,

$$\left(\frac{\omega}{\omega_o}\right)_B^2 = 1 - \frac{\Gamma}{\Gamma_B} + 3\Psi^2 - \psi_1^2 + \frac{\Gamma_T}{\Gamma_B}(\Phi^2 - \phi_1^2) - \frac{I_{10}}{\omega_{o_B} I_9} \qquad (8)$$

$$\left(\frac{\omega}{\omega_o}\right)_T^2 = 1 - \frac{\Gamma}{\Gamma_T} + 3\Phi^2 - \phi_1^2 + \frac{\Gamma_B}{\Gamma_T}(\Psi^2 - \psi_1^2) - \frac{I_{10}}{\omega_{o_T}^2 I_9} \qquad (9)$$

Since ψ_1, ϕ_1, Γ, and I_{10} are specified quantities, it is only necessary to find Φ and Ψ in order to calculate the frequencies. Setting the inertial terms equal to zero in equations (6) and (7) yields the static deflection equations,

$$\Psi^3 + \Psi\left[1 - \frac{\Gamma}{\Gamma_B} - \psi_1^2 + \frac{\Gamma_T}{\Gamma_B}(\Phi^2 - \phi_1^2) - \frac{I_{10}}{\omega_{o_B}^2 I_9}\right] = \psi_o + \psi_1 \qquad (10)$$

$$\Phi^3 + \Phi\left[1 - \frac{\Gamma}{\Gamma_T} - \phi_1^2 + \frac{\Gamma_B}{\Gamma_T}(\Psi^2 - \psi_1^2) - \frac{I_{10}}{\omega_{o_T}^2 I_9}\right] = \phi_o + \phi_1 \qquad (11)$$

Therefore, the problem reduces to that of finding Φ and Ψ from the above two equations and then substituting these results into equations (8) and (9) to get the effects on stiffness. A parametric study has been made of equations (10) and (11) for values of Γ/Γ_T from 0 to 2.0 and for various combinations of the parameters ψ_1, ϕ_1, and $\Gamma_T/\Gamma_B = \frac{\Delta T_T}{\Delta T_B}$, (see Appendix III).

Results

First, the experimental data recorded at the Air Force Institute of Technology are shown in Figures 5, 6, 8, and 9. ψ_1 and ϕ_1 are not known, but the ratio $\Delta T_B/\Delta T_T$ for the rectangular plate, Fig. 5, was calculated as 1.029. Note that the first mode frequency increases while the second mode frequency levels off. Fig. 6 shows the same phenomena for a slightly tapered plate.

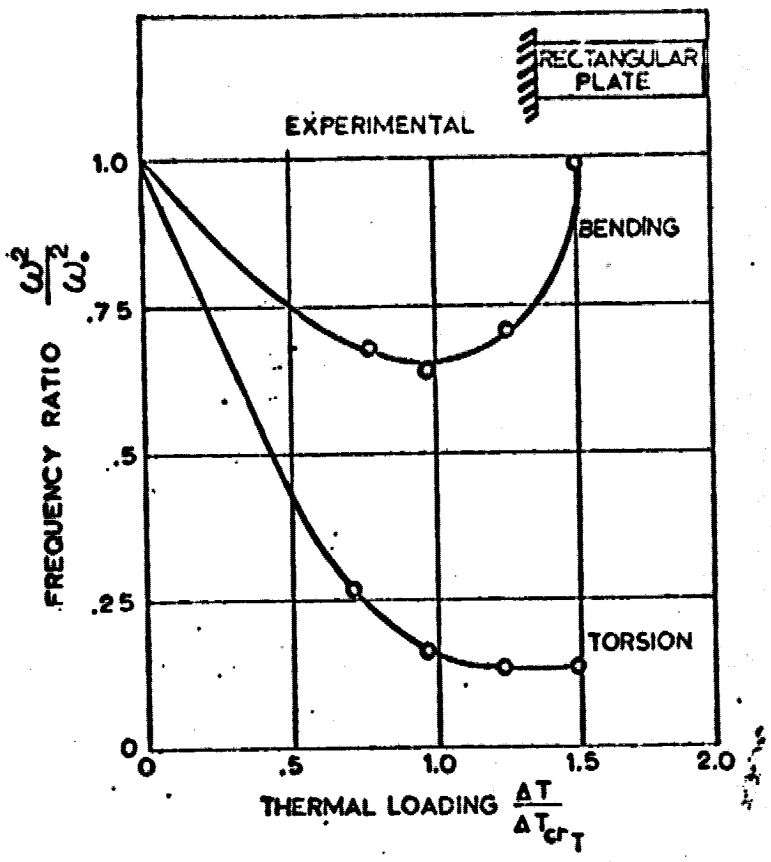

Fig. 5. Frequency Response With Coupling

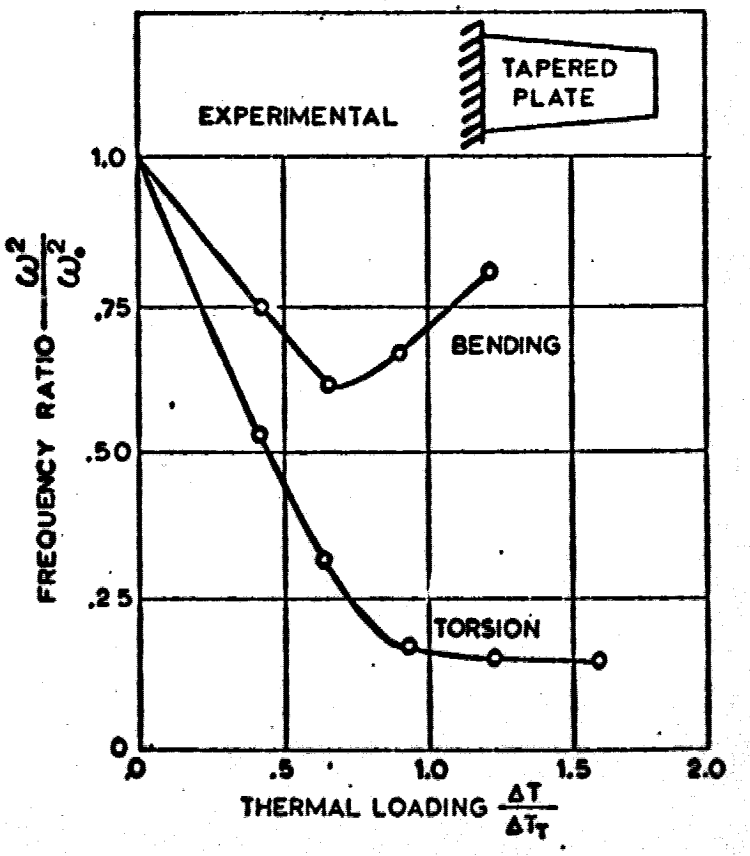

Fig. 6. Frequency Response With Coupling

Figure 7 shows the predicted response for the coupled first and second modes for a plate for which,

$$\frac{\Delta T_B}{\Delta T_T} = 1.0, \quad \phi_i = 0.02, \quad \psi_i = 0.1$$

$$\psi_o = \phi_o = I_{10} = 0$$

The first mode frequency increases after buckling while the second mode levels off, just as in the experiment.

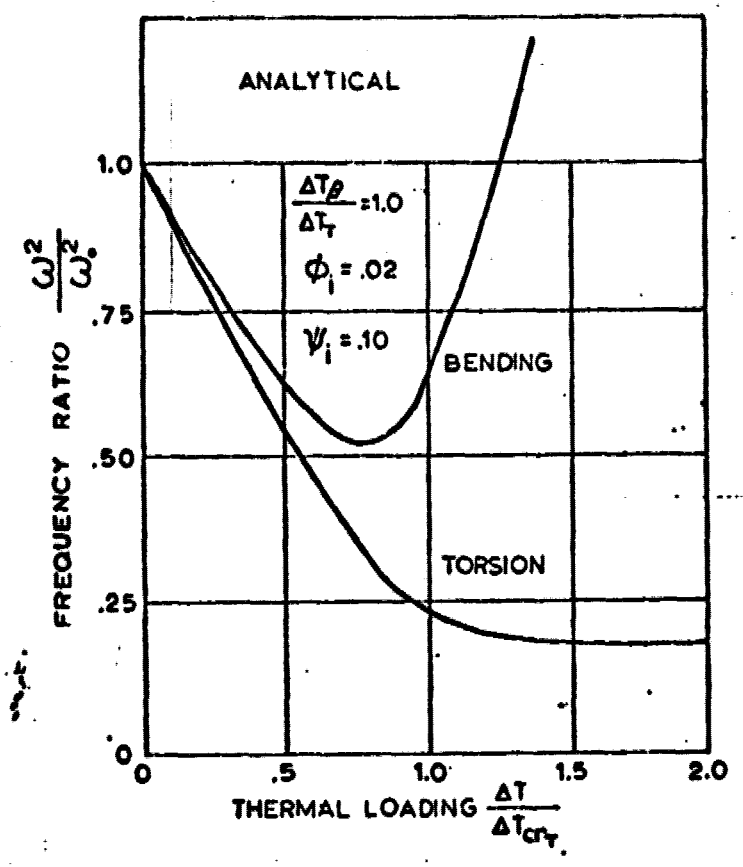

Fig. 7. Frequency Response With Coupling

Figure 8 and Figure 9 show the experimental results for highly tapered plates of the same aspect ratio and thickness as the previous plates. For these plates, the second mode frequency increases in the conventional manner while the first mode levels off. Again, ψ_i and ϕ_i are not known for the plates but a ratio of $\Delta T_B/\Delta T_T = 1.072$ has been calculated from linear theory.

Figure 10 shows that for $I_B/I_T = 1.1$ the analytical response has the same trend as the experimental data. Since the slope of the response curves is affected by the initial imperfection for a given $\Delta T_B/\Delta T_T$, extrapolation of experimental data to obtain ΔT_B and ΔT_T is likely to lead to erroneous results.

A comparison of theoretical to experimental results from Reference 2 is shown in Figure 3. The theoretical curve does not contain any effect of initial deformation in the bending mode, although the initial plate shape, Figure 2, indicates

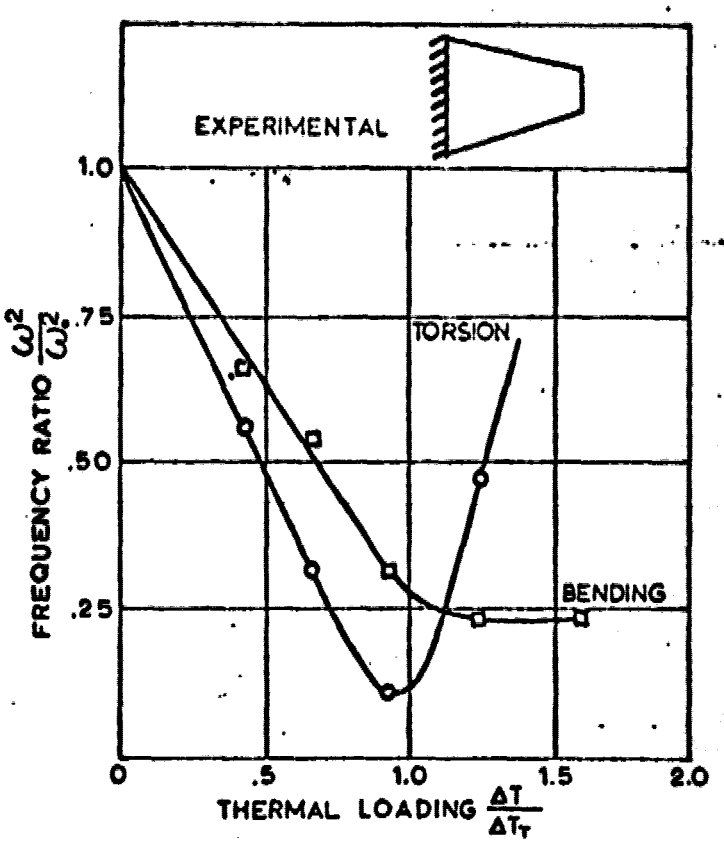

Fig. 8. Frequency Response With Coupling

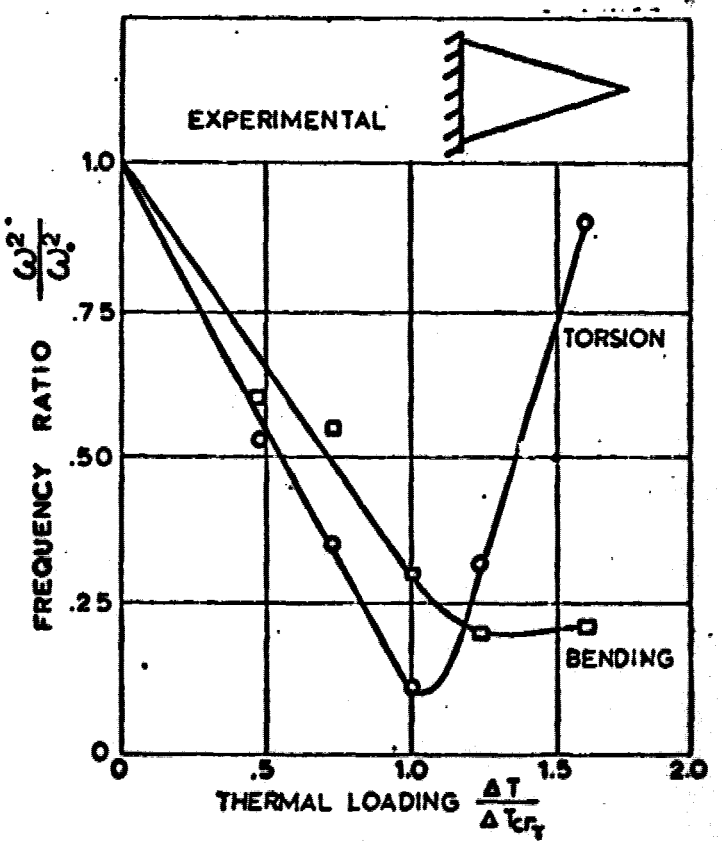

Fig. 9. Frequency Response With Coupling

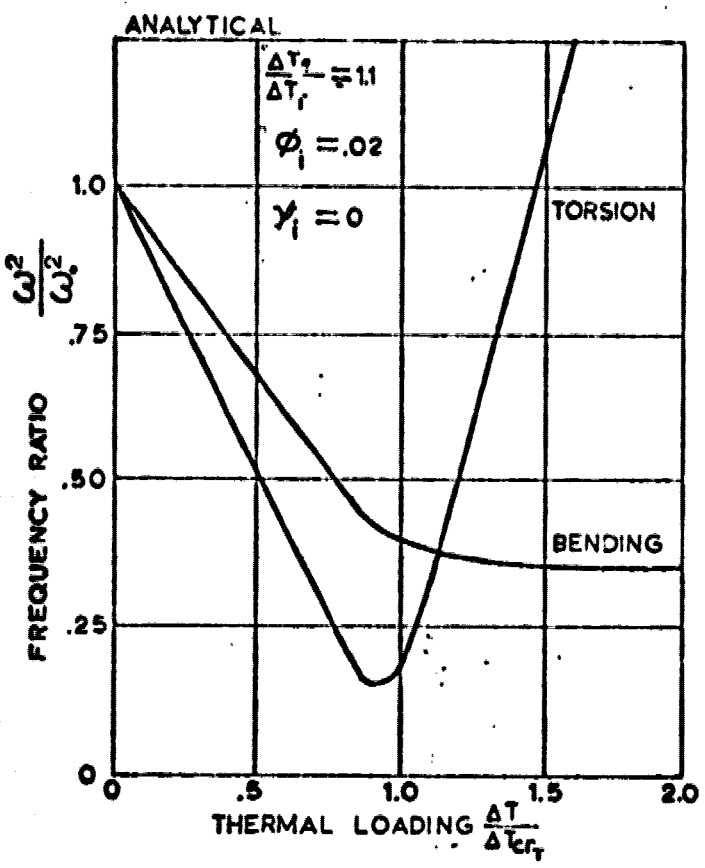

Fig. 10. Frequency Response With Coupling

quite large bending and camber. Thus, the effect of finite ψ_1 could not be eliminated from the experimental data.

Figure 11 shows two curves for $\Delta T_B/\Delta T_T = 1.1$. The first curve is for $\phi_1 = 0.06$ (about the correct value), and $\psi_1 = 0$, which would be representative of the analytical curve in Figure 3. The second curve in Figure 11 occurs when $\psi_1 = 0.2$ and would be representative of the experimental curve in Figure 3 which may explain in part the disagreement between experiment and theory in Reference 2.

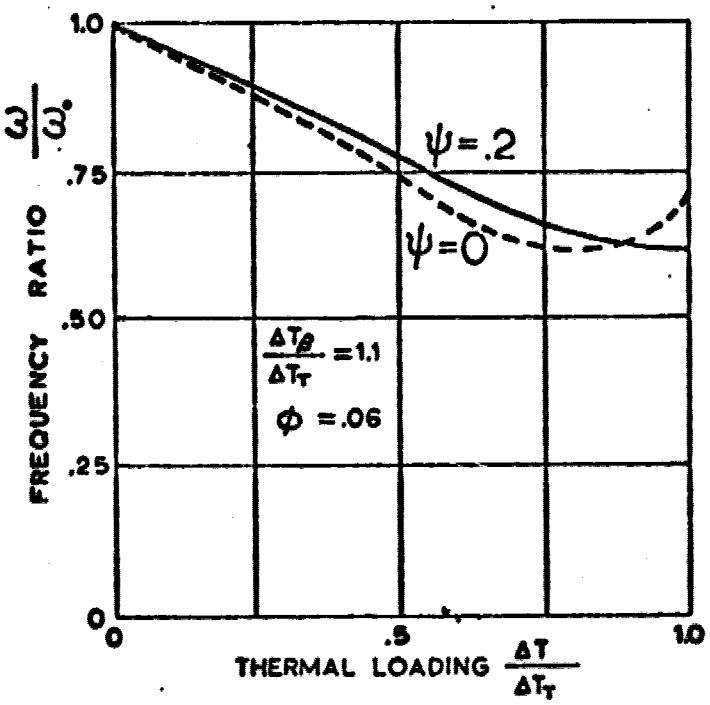

Fig. 11. Frequency Response With Coupling

Conclusions

Both experimental and analytical data indicates strong coupling between the first two modes of plates with in-plane stresses. The onset of significant coupling varies with the initial imperfections and with the ratio of in-plane buckling parameters, $\Delta T_B/\Delta T_T$.

The post buckling behavior of plates for which $\Delta T_B/\Delta T_T \neq 1$, is determined by the ratio $\Delta T_B/\Delta T_T$. If $\Delta T_B/\Delta T_T$ is sufficiently less than 1, the second mode frequency will always level off and the first mode frequently will increase, whereas for $\Delta T_B/\Delta T_T$ sufficiently greater than 1, the first mode will level off and the second mode will increase. For $\Delta T_B/\Delta T_T$ sufficiently close to 1, the relative magnitudes of the initial imperfections will determine which mode levels off and which mode increases.

The small amplitude vibration frequency about the large amplitude static equilibrium position is independent of planform shape, boundary conditions, thickness distribution and temperature distribution except as these factors affect the thermal buckling parameters.

Appendix I

The I_i are nine integrals of known functions over the plate surface and are known quantities from the linear solution.

$$I_1 = \iint \rho t W_1^2 dxdy$$

$$I_2 = \iint D\{(\frac{\partial^2 W_1}{\partial x^2})^2 + (\frac{\partial^2 W_1}{\partial y^2})^2 + 2\nu \frac{\partial^2 W_1}{\partial x^2} \frac{\partial^2 W_1}{\partial y^2} + 2(1-\nu)(\frac{\partial^2 W_1}{\partial x \partial y})^2\} dxdy$$

$$I_3 = \iint t\{\frac{\partial^2 G}{\partial x^2}(\frac{\partial W_1}{\partial y})^2 + \frac{\partial^2 G}{\partial y^2}(\frac{\partial W_1}{\partial x})^2 - \frac{\partial^2 G}{\partial x \partial y} \frac{\partial W_1}{\partial x} \frac{\partial W_1}{\partial y}\} dxdy$$

$$I_4 = \iint Z W_1 \, dxdy$$

$$I_5 = \iint \rho t W_2^2 \, dxdy$$

$$I_6 = \iint D\{(\frac{\partial^2 W_2}{\partial x^2})^2 + (\frac{\partial^2 W_2}{\partial y^2}) + 2\nu \frac{\partial^2 W_2}{\partial x^2} \frac{\partial^2 W_2}{\partial y^2} + 2(1-\nu)(\frac{\partial^2 W_2}{\partial x \partial})\}^2 \, dxdy$$

$$I_7 = \iint t\left(\frac{\partial^2 G}{\partial x^2}\left(\frac{\partial W_2}{\partial y}\right)^2 + \frac{\partial^2 G}{\partial y^2}\left(\frac{\partial W_2}{\partial x}\right)^2 - 2\,\frac{\partial^2 G}{\partial x \partial y}\,\frac{\partial W_2}{\partial x}\,\frac{\partial W_2}{\partial y}\right) dxdy$$

$$I_8 = \iint Z\, W_2\, dxdy$$

$$I_9 = \iint \frac{t}{E}\left(\left(\frac{\partial^2 G}{\partial x^2}\right)^2 + \left(\frac{\partial^2 G}{\partial y^2}\right)^2 - 2\nu\,\frac{\partial^2 G}{\partial x^2}\,\frac{\partial^2 G}{\partial y^2} + 2(1-\nu)\left(\frac{\partial^2 G}{\partial x \partial y}\right)^2\right) dxdy$$

$$I_{10} = \int t\left(\frac{\partial^2 G}{\partial x^2}\,V + \frac{\partial^2 G}{\partial y^2}\,U\right) ds$$

$$r = \iint t\, T(x,y,\tau)\left(\frac{\partial^2 G}{\partial x^2} + \frac{\partial^2 G}{\partial y^2}\right) dxdy$$

Appendix II

The equations of motion are:

$$\frac{\ddot{\psi}}{\omega_{o_B}^2} + \psi^3 + \psi\left[1 - \frac{r}{r_B} - \psi_i^2 + \frac{r_T}{r_B}(\phi^2 - \phi_i^2) - \frac{I_{10}}{\omega_{o_B}^2 I_9}\right] = \psi_o + \psi_i$$

$$\frac{\ddot{\phi}}{\omega_{o_T}^2} + \phi^3 + \phi\left[1 - \frac{r}{r_T} - \phi_i^2 + \frac{r_B}{r_T}(\psi^2 - \psi_i^2) - \frac{I_{10}}{\omega_{o_T}^2 I_9}\right] = \phi_o + \phi_i$$

Assume:

$$\psi = c_\psi + \nu$$
$$\phi = c_\phi + \phi$$

Substitute:

$$\frac{\ddot{c}_\psi}{\omega_{o_B}^2} + (c_\psi+\nu)^3 + [c_\psi+\nu]\left[1 - \frac{r}{r_B} - \psi_i^2 + \frac{r_T}{r_B}((c_\phi+\phi)^2 - \phi_i^2) - \frac{I_{10}}{\omega_{o_B}^2 I_9}\right] = \psi_o + \psi_i$$

$$\frac{\ddot{c}_\phi}{\omega_{o_T}^2} + (c_\phi+\phi)^3 + [c_\phi+\phi]\left[1 - \frac{r}{r_T} - \phi_i^2 + \frac{r_B}{r_T}((c_\psi+\nu)^2 - \psi_i^2) - \frac{I_{10}}{\omega_{o_T}^2 I_9}\right] = \phi_o + \phi_i$$

neglect all 2nd and higher order terms in c and neglect $2c_\psi/\nu$ and $2c_\phi/\phi$ compared to unity. Subtract away the static deflection equation in each case to obtain:

$$\frac{\ddot{c}_\psi}{\omega_{o_B}^2} + \left[1 - \frac{r}{r_B} + 3\nu^2 - \psi_i^2 + \frac{r_T}{r_B}(\phi^2 - \phi_i^2) - \frac{I_{10}}{\omega_{o_B}^2 I_9}\right] c_\psi = 0$$

$$\frac{\ddot{c}_\phi}{\omega_{o_T}^2} + \left[1 - \frac{r}{r_T} + 3\phi^2 - \phi_i^2 + \frac{r_B}{r_T}(\nu^2 - \psi_i^2) - \frac{I_{10}}{\omega_{o_T}^2 I_9}\right] c_\phi = 0$$

Assume that the small amplitude vibration will be simple harmonic (experimental evidence supports this assumption). The equations from which the frequency may be obtained result:

$$\left(\frac{\omega}{\omega_o}\right)_B^2 = 1 - \frac{r}{r_B} + 3\nu^2 - \psi_i^2 + \frac{r_T}{r_B}(\phi^2 - \phi_i^2) - \frac{I_{10}}{\omega_{o_B}^2 I_9}$$

$$\left(\frac{\omega}{\omega_o}\right)_T^2 = 1 - \frac{r}{r_T} + 3\phi^2 - \phi_i^2 + \frac{r_B}{r_T}(\nu^2 - \psi_i^2) - \frac{I_{10}}{\omega_{o_T}^2 I_9}$$

Appendix III

The thermal loading term, r, occurs as:

$$r = \iint \alpha t T(x,y,\tau)(\sigma_x + \sigma_y) dxdy$$

Assume that the surface temperature function $T(x,y,\tau)$ may be written relative to some reference value ΔT_{ref} or:

$$T(x,y,\tau) = \Delta T_{ref}(\tau)\, f(x,y)$$

Thus:

$$r = \Delta T_{ref} \iint \alpha t\, f(x,y)(\sigma_x + \sigma_y) dxdy$$

and

$$r_{critical} = \Delta T_{ref\ critical} \iint \alpha t\, f(x,y)(\sigma_x + \sigma_y) dxdy$$

Thus:

$$\frac{r}{r_{critical}} = \frac{\Delta T_{ref}}{\Delta T_{ref(critical)}}$$

Also:

$$\frac{r_B}{r_T} = \frac{\Delta T_{ref(critical)first\ mode}}{\Delta T_{ref(critical)second\ mode}} = \frac{\Delta T_B}{\Delta T_T}$$

References

1. Reissner, E., "On a Variational Theorem for Finite Elastic Deformations," Journal Mathematics and Physics, Vol. XXXII, Nos. 2-3, July-October 1953, p. 129.

2. Heldenfels, R. R., and Vosteen, L. F., "Approximate Analysis of Effects of Large Deflections and Initial Twist on Torsional Stiffness of a Cantilever Plate Subjected to Thermal Stresses," NACA Report 1361, 1958, Supersedes NACA TN 4067, 1957.

3. Bailey, C. D., "Vibration and Buckling of Thermally Stressed Plates of Trapezoidal Planform," Ph.D. Dissertation, Purdue University, January 1962.

4. Breuer, D. W., "Effects of Finite Displacement, Aspect Ratio and Temperature on the Torsional Stiffness of Cantilever Plates," Fourth U.S. National Congress of Applied Mechanics.